Exciton–Exciton Interaction and Optical Gain in Colloidal CdSe/CdS Dot/Rod Nanocrystals

By *Michele Saba,* Stefan Minniberger, Francesco Quochi, Juergen Roither, Marco Marceddu, Agnieszka Gocalinska, Maksym V. Kovalenko, Dmitri V. Talapin, Wolfgang Heiss, Andrea Mura,* and *Giovanni Bongiovanni*

Semiconductor colloidal nanocrystals have been proposed as optically-active media for solution-processable optoelectronic devices, because they combine inexpensive, wet-chemistry synthesis with high photoluminescence quantum yield, large oscillator strength and size tuneability of optical transitions.[1–4] Key to the success of nanocrystal-based devices is the possibility to design and consistently synthesize nanocrystals with desired properties. Size uniformity can be usually controlled within less than 5% uncertainty; surface capping, passivation and core/shell structures can lead to photoluminescence quantum yields exceeding 50%, optical gain and lasing.[5]

A new frontier in nanocrystal design has appeared with heterostructures allowing spatial separation of electron and hole wavefunctions, like in type-II CdSe/CdTe core/shell nanocrystals, through staggered conduction and valence band offsets.[6,7] Charge separation inside nanocrystals is useful in photodetector and photovoltaic devices, quantum optics and low-threshold lasers. Exciton nonlinearities also depend on the degree of separation of electron and hole wavefunction. In type-II heterostructures, it has been demonstrated that charge separation can lead to a large repulsive exciton–exciton interaction. The resulting blueshift of the exciton-to-biexciton transition suppresses to a large extent resonant re-absorption of stimulated emission from single-exciton states, allowing net optical gain and lasing at excitations corresponding to less than one electron-hole pair per nanocrystal. In this regime, losses inherent to multi-exciton recombinations are avoided, resulting in optical gain with a much longer lifetime, an essential step towards the demonstration of lasing under continuous wave operation.

CdSe/CdS dot/rod nanocrystals represent a recently developed class of heterostructures, formed by a spherical CdSe core, subsequently covered by a rod-shaped CdS shell (scheme in Fig. 1a).[8–11] While bulk CdSe and CdS have in principle a type-I band alignment, with CdSe band energies both enclosed within CdS ones, the two conduction bands are so close to each other that conduction electron wavefunctions can significantly spread into the rod (Fig. 1c), realizing what is sometimes referred to as a quasi-type-II heterostructure. Electronic states in dot/rods nanocrystals can be confined in either zero or one dimension, a property that can be suitably exploited for many optoelectronic applications: an applied electric field has been shown to control emission wavelength and exciton lifetime[12,13] and has even allowed storage of excitons in dark states for long transients.[14] Thanks to its huge absorption cross-section, the CdS shell efficiently absorbs light and funnels the photoexcitation into the quantum dot. If successfully combined with repulsive exciton–exciton interaction, this feature could reduce the threshold for achieving gain in the single exciton regime by several orders of magnitude with respect to spherical, type-II core/shell nanocrystals.

In this work we set to determine exciton–exciton interaction and optical gain in CdSe/CdS dot/rod nanocrystals.[8,9] We examined 4 different batches of nanocrystals, with length along the rod axis ranging from around 30 nm to over 50 nm, as visible in the TEM images in Figure 1b. The main morphology difference between batches could be found on the girth in the vicinity of the CdSe dots, as samples #1 and #2 showed a pronounced CdS bump, while in samples #3 and #4 the rod shape was regular, without bumps. Linear optical properties were found to be similar for all 4 samples batches, as expected from similar nanocrystal shapes and compositions. The optical absorption spectra were all characterized by very large molar extinction factors (in excess of 10^7 $mol^{-1}\,cm^{-1}$ around 400 nm in wavelength) and were dominated by CdS features, with only shoulders around 600 nm signaling the presence of CdSe, consistent with the fact that CdSe occupied only a few percent of the nanocrystal volume (Fig. 1d). On the contrary, continuous wave (cw) luminescence was emitted almost exclusively around the CdSe bandgap energy and the quantum yield was higher than 70% at all optical excitation energies, meaning that most photogenerated excitations relaxed to the lowest energy allowed by the CdSe/CdS heterostructure. A very narrow-size dispersion of the nanocrystal samples reflected into 30–40 nm FWHM for photoluminescence. Only in sample #3 we found an asymmetric photoluminescence lineshape, probably due to contributions from spurious species.

To access photoluminescence dynamics, the emission was time-resolved with a streak camera, after exciting solutions of

[*] Dr. M. Saba, Dr. F. Quochi, Dr. M. Marceddu, A. Gocalinska, Prof. A. Mura, Prof. G. Bongiovanni
Dipartimento di Fisica and SLACS-CNR/INFM, Università di Cagliari
09042 Monserrato (Italy)
E-mail: michele.saba@dsf.unica.it
S. Minniberger, Dr. J. Roither, Prof. W. Heiss
Institute of Semiconductor and Solid State Physics
Johannes Kepler University
Altenbergerstr. 6g, 4040 Linz (Austria)
Dr. M. V. Kovalenko, Prof. D. V. Talapin
Department of Chemistry, The University of Chicago
Chicago, IL 60637 (USA)

DOI: 10.1002/adma.200901482

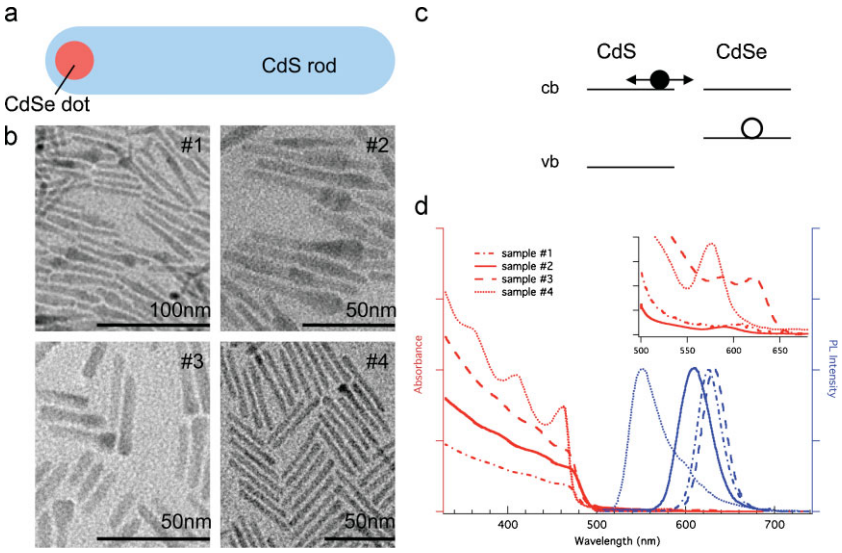

Figure 1. a) Sketch of the dot/rod nanocrystal structure. b) TEM pictures of the four different nanocrystal types we studied. Samples #1 and #2 appeared to have a bump corresponding to the CdSe dot location, while samples #3 and #4 showed a more regular shape across all rod length. c) Sketch of band alignment at the CdS/CdSe heterostructure interface. d) Nanocrystal absorption (red lines, left axis) and cw-photoluminescence spectra (blue line, right axis); different line styles correspond to different samples, as in the legend; the same line style is used for absorbance and luminescence for each sample; the inset reports a magnification of absorbance in the low-energy tail.

nanocrystals dispersed in toluene with sub-picosecond laser pulses. The excitation level, or average number of excitons $\langle N \rangle$ created in each nanocrystal, was calculated multiplying the laser photon density Φ with the absorption cross-section σ for the nanocrystals at the laser wavelength ($\sigma = 5.4 \times 10^{-14}\,\mathrm{cm}^{-2}$ at 394 nm).[9] The spectrogram in Figure 2a refers to sample #1, was taken at very low excitation levels and showed that the emission from the CdSe dot decayed with a ~20 ns single exponential time, while a very weak trace of emission from the CdS rod was visible only at early times after excitation and decayed within the time resolution. The long decay of dot emission in such CdSe/CdS heterostructures, compared to bare CdSe or CdSe/ZnS nanocrystals of similar size, has been linked to the reduced electron/hole overlap and consequent reduction in oscillator strength for the excitonic transition.[9,15] The fast decay of the rod emission could be attributed to hot exciton emission. Similarly long exciton decay times were found in all 4 samples (see Supporting Information).

The spectrogram evolved significantly for high excitation levels (Fig. 2b), when each nanocrystal was injected with more than one exciton on average. At early times after excitation and for all considered nanocrystals, the emission from the rod became comparable in intensity to the emission from the dot. At high excitation densities and time 0, additional optical emission appeared at energies higher than exciton transitions, but still much lower than the CdS rod gap, which we attributed to higher excited, multiexciton states in the CdSe core.[10,16,17] The large broadening of the peak might be an indication of further delocalization of conduction electrons across the rod for such excited states. Emission at the exciton energy in CdSe dots became much faster at higher excitation fluences, a clear indication of multiexciton recombination. The lifetime of biexciton states was estimated to be ~330 ps by fitting photoluminescence time decays for various excitation intensities with a double exponential (very similar dynamics were measured in all samples, see Supporting Information).[18] However the decay time for the long excitonic component depended on the excitation power, becoming faster for higher excitation levels (see Supporting Information).

Differences among various nanocrystals were apparent in the spectral evolution of the exciton peak with increasing excitation fluence. Figure 3 summarizes the comparison of spectra measured immediately after the arrival of the excitation pulse in the linear and multiexciton regimes (a gate window of 50 ps was selected). A shift appeared in the peak wavelength for the dot emission, which measured the exciton–exciton interaction energy. The observed shift varied from 31 meV to the blue (in sample #2), to 20 meV to the blue (sample #1), to 4.5 meV to the red (samples #3), to 3.6 meV to the red (sample #4), indicating that exciton–exciton interaction could be tuned from attractive (corresponding to a redshift of biexciton transitions with respect to exciton ones, as in conventional core/shell nanocrystals) to repulsive (biexciton is blueshifted with respect to exciton) with minor nanocrystal shape modifications. Nanocrystals with increased girth around the CdSe dot showed exciton–exciton repulsion, which could be attributed to larger spatial separation between electrons and holes, as electrons had a thicker CdS shell to spread into. On the other hand, in nanocrystals without the bump around the CdSe core electrons found a very thin CdS shell in all directions except the rod long axis, so that spreading outside the dot of electron wavefunctions was reduced, resulting in a weak exciton–exciton attraction.[19]

A complementary tracking of exciton dynamics was provided by a transient absorption experiment, a technique sensitive to bleaching from single carriers (a single electron or hole affects absorption), while photoluminescence gave information only on the joint population of electrons and holes. Figure 4a shows the differential transmission spectrum at 1 ps delay between pump and probe pulses in sample #1: it appeared that even at excitation intensities creating less than one exciton per nanocrystal, a differential transmission signal was present both at the wavelength of the dot emission and that of the rod emission, a feature common to all measured nanocrystals. The spectrogram (Fig. 3b) and the differential transmission decay curves (Fig. 3d) showed that both rod and dot signals had similar decay rates, with typical times longer than our 0.5 ns observation window.[15] Given that, under the same conditions, very little luminescence was emitted at the rod transition energy, the observation of bleaching for probe wavelengths below 500 nm was consistent with the electrons being significantly delocalized over the rod and therefore affecting also CdS transitions. A blow-up of the differential signal dynamics just after the arrival of the excitation

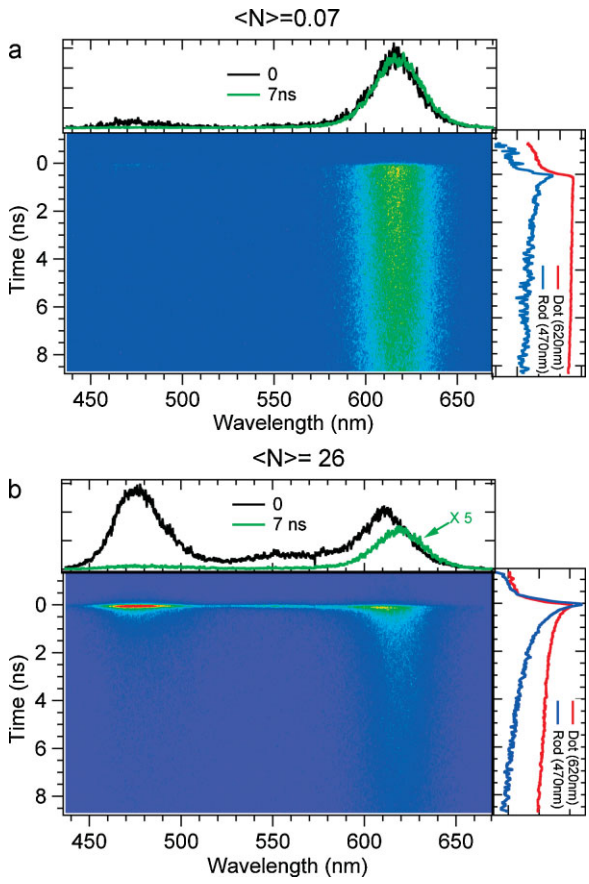

Figure 2. a) Time-resolved photoluminescence spectrogram (spectrum as a function of time) at low excitations (linear regime), corresponding to 0.07 excitons/dot on average. The upper inset shows two spectral cuts, the black one around 0 delay (50 ps window), the green one at 7 ns (1 ns window). The right panel shows in log scale the temporal evolution of the dot (red line, signal at 620 nm, integrated over a 20 nm window) and rod (blue line, signal at 470 nm, integrated over a 20 nm window). b) Spectrogram at high excitations, corresponding to 26 excitons/dot on average. Upper and side panels were obtained like in (a).

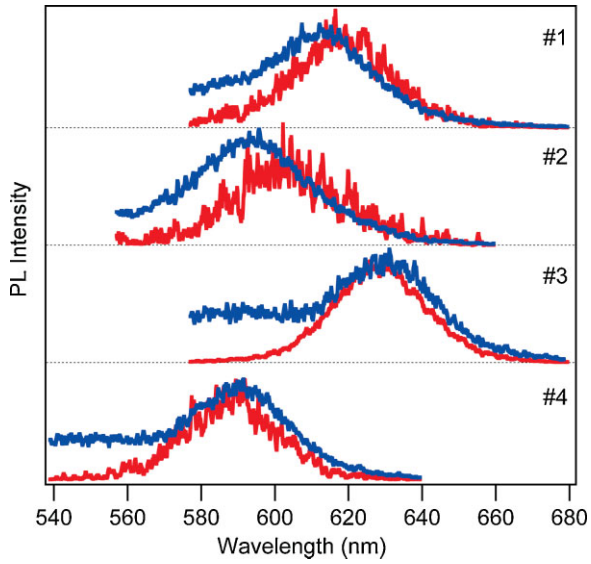

Figure 3. PL spectra in the high-excitation (blue lines) and linear regimes (red lines) for the samples we considered. Spectra are integrated over a 50 ps window starting with the excitation pulse arrival (the gate duration was chosen shorter than biexciton lifetime). The intensity is given in arbitrary units; vertical offsets have been added for clarity. The shift of the biexciton transition with respect to the exciton one is 20 meV for sample #1, 30 meV for sample #2, −3.6 meV for sample #3, −4.5 meV for sample #4.

pulse (inset in Fig. 3c) hinted at a picosecond rise time for the dot signal, which could be related to the time needed to capture carriers from the rod into the dot.[20]

The ratio of the differential transmission signal at the rod and dot transition wavelengths has been shown to provide a measure of charge separation in dot/rod nanocrystals,[20] as the rod signal grows with growing penetration of electron wavefunctions inside the rod shell. In the four samples we measured, the ratio of dot-to-rod differential transmission signals varied and turned out to be correlated to the exciton binding energy: the samples with repulsive exciton–exciton interaction showed a larger rod signal (13 and 7 times larger than the dot signal, respectively, for samples #1 and #2) with respect to the samples with attractive interaction (for both samples #3 and #4 the ratio was around 4). Such observation was consistent with the interpretation we gave of exciton–exciton interaction and demonstrated once more that electron confinement in such asymmetric nanocrystals critically depends on shape details around the CdSe dot. Our finding may help reconciling conflicting conclusions reported on electron localization from different experiments on CdSe/CdS dot/rod nanocrystals.[20,21]

At higher excitation levels, the differential transmission signal at the rod energy increased much more than the one at the dot energy, similarly to what happened for the photoluminescence signal. In the nonlinear regime, the decays of the dot and rod signals departed significantly from each other: the rod signal decay became much faster and nonexponential, an apparent consequence of multiparticle Auger effects.

A detailed comparison of excitation power dependence of both luminescence and differential absorption allowed quantitative estimates of the number of excitons contained in nanocrystals. The peak value of the luminescence signal from streak images (both for dot and rod signals and for a reference sample of commercial core/shell CdSe/ZnS nanocrystals emitting at 620 nm) has been plotted as a function of the average number $\langle N \rangle$ of excitons injected in the nanocrystal (Fig. 4e). When $\langle N \rangle \ll 1$, the peak luminescence signal was proportional to $\langle N \rangle$ (linear regime). Assuming that luminescence from the dot was the only relaxation channel for injected excitons in the linear regime, the slope for the dot-luminescence signal in the linear regime was normalized to 1, so that the photoluminescence intensity value around 2 obtained at saturation measured the maximum occupation in the lowest exciton state (the peak value is obtained integrating over exciton and biexciton emission), consistent with the double degeneracy of the conduction band. A very similar photoluminescence saturation was observed for commercial core/shell CdSe/ZnS round nanocrystals.[22] The rod photoluminescence signal on the contrary kept growing with the excitation power (even superlinearly in a small regime), meaning that many excitons could be stored inside each rod. The red line in Figure 4e is not a fit to the data, but a theoretical prediction for the

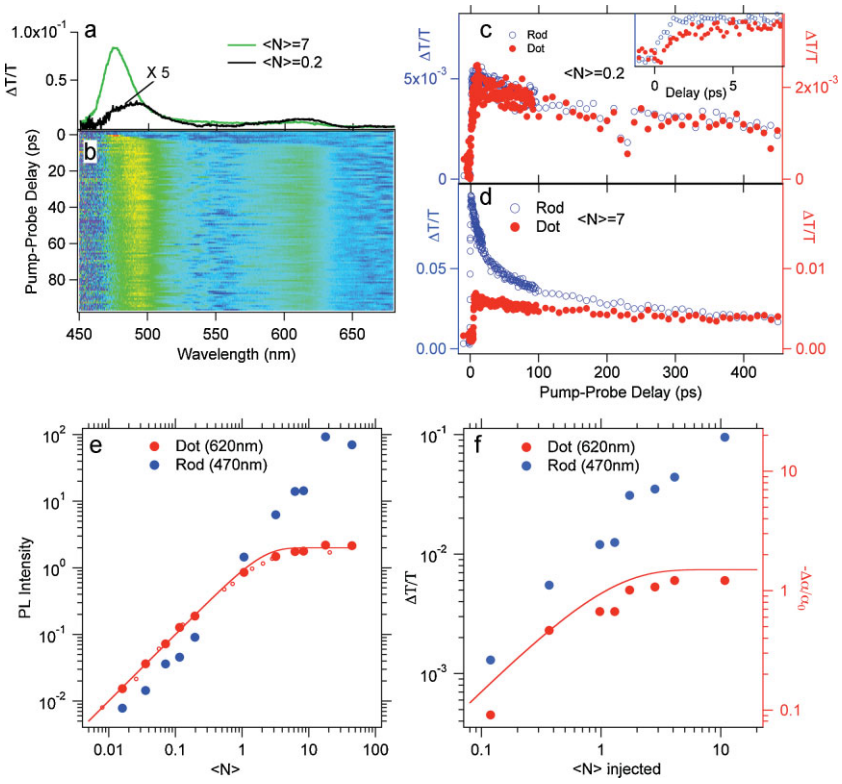

Figure 4. Pump-probe experiments on sample #2. a) Differential transmission spectra at 1 ps pump-probe delay, low (black line) and high (green line) excitation levels. b) Differential transmission spectrogram (spectrum as a function of the pump-probe delay). The tilt of the zero line as a function of wavelength is due to the chirp of the white light pulses; the effect is corrected in the profile plots. c) Evolution of the differential transmission signal at the dot (red dots, 610 nm) and rod (blue dots, 470 nm) wavelengths as a function of the pump-probe delay; the excitation level corresponds to less than 1 exciton per dot ($\langle N\rangle = 0.2$). The inset shows the same data on a more limited scale to highlight the rise time for the dot signal. d) Same as (c), but for a high excitation level (7 excitons per dot on average). e) Photoluminescence peak intensity as a function of the excitation intensity at dot transition (solid red dots), rod transition (blue dots) and for the exciton transition in commercial core/shell CdSe dots (empty red dots). The red line is the Poisson saturation as explained in the text. f) Differential transmission peak signal at rod and dot energies as a function of the excitation intensity. The left axis is calibrated in units of the relative differential absorption for the dot transition. The red line is a prediction for differential absorption based on the assumption that exciton repulsion is much larger than transition linewidth (see text).

number of excitons n inside a dot $n = 2 - e^{-\langle N\rangle}(\langle N\rangle + 2)$, obtained assuming only that excitons are injected with average number $\langle N\rangle$ according to Poisson distribution (the probability of finding n excitons in a nanocrystal is $P(n) = \frac{\langle N\rangle^n e^{-\langle N\rangle}}{n!}$) and that each nanocrystal could contain a maximum of 2 excitons in its lowest doubly degenerate state.

The evolution of the peak value of the differential absorption signal as a function of $\langle N\rangle$ (Fig. 4f) also showed that the signal from the dot saturated for growing excitation intensities, while the signal from the rod kept increasing. To calibrate the magnitude of the differential signal from the dot, we divided the differential absorption $-\Delta\alpha$ by the linear absorption α_0 at the corresponding wavelength, so that $0 < -\Delta\alpha/\alpha_0 < 1$ meant that bleaching of the transition occurred, while $-\Delta\alpha/\alpha_0 > 1$ was the conditionn for optical gain. The differential absorption for the dot signal saturated at a value above 1 and optical gain occurred for $\langle N\rangle$ close to 1. The statistical error on $-\Delta\alpha/\alpha_0$ was however of the order of 10%, owing to the uncertainty on the small values of both $\Delta\alpha$ and α_0 at the dot transition. Thanks to the very high absorption cross-section of dot/rod nanocrystals, the gain threshold was reached for an extremely low pump fluence, ~10 μJ cm^{-2}, more than 100 times lower than the gain threshold reported for type-II nanocrystals.[7] With such a low threshold comes also a low absolute value for optical gain itself, so that in a working laser device based on dot/rod nanocrystals special care will have to be taken to limit optical losses.

A simple theoretical prediction for differential absorption in the limit that the biexciton repulsion energy Δ is larger than the exciton emission linewidth Γ, is that: $\frac{-\Delta\alpha}{\alpha_0} = \frac{3}{2}\left(1 - e^{-\langle N\rangle}\right)$ (red line in Fig. 4f); in our case, however, the benefit of exciton repulsion was limited by the fact that Γ was about three times larger than Δ, so that the optical gain could be therefore predicted to occur for $\langle N\rangle_{th} = \frac{2}{3 - e^{-\Delta^2/\Gamma^2}} \cong 0.95$.[7] An even lower gain threshold could be achieved by further optimization of nanocrystal design: smaller CdSe cores, for example, or thicker rod shells surrounding them, may lead to greater charge separation and larger biexciton repulsion. As an added benefit, the exciton lifetime τ_X at gain threshold would increase from 1 ns (the value we measured for $\langle N\rangle \sim 1$) towards 20 ns (the value we measured in the linear regime for $\langle N\rangle \ll 1$). The corresponding optical pumping density P_{th}, needed to maintain inversion in cw conditions, is given by $P_{th} = \langle N\rangle_{th}\frac{\hbar\omega}{\sigma\tau_X}$, so that both a long exciton lifetime τ_X and the large absorption cross-section σ due to the antenna effect of the rod contribute to keep P_{th} low; its value would therefore jump from approximately 10 kW cm^{-2} (for $\tau_X = 1$ ns and $\sigma = 10^{15}$ cm^2) down to 500 W cm^{-2} (for $\tau_X = 20$ ns), a value compatible with indirect optical pumping with a blue diode, as demonstrated for polymer lasers.[23]

In conclusion, ultrafast nonlinear spectroscopy revealed that exciton–exciton interaction in CdSe/CdS dot/rod nanocrystals can be sensitively tuned, from attractive to repulsive, with minor modifications in the nanocrystal shape. Exciton–exciton repulsion is a very beneficial feature to achieve lasing under cw or quasi-cw pumping, especially when coupled with the antenna effect provided by the CdS rod and the large photoluminescence quantum yield. Present experimental results validate the use of CdSe/CdS dot/rod nanocrystals as materials of choice to combine ultra-low gain threshold with long lifetime gain. The prospects of CdSe/CdS colloidal heterostructures are further enhanced by the rich variety of structure sizes and shapes that can be synthesized,[24] including smaller CdSe dots that could enhance the repulsive excitonic interaction and multibranched CdS arms that attach to zincblende-phase CdSe dots.

Experimental

Nanocrystal Preparation: CdSe/CdS dot-rod samples were grown and purified according to previously published protocol (Ref.[9]). Special care was taken to remove traces of tetrapods by means of size-selective precipitation. The smoothness of the rods was varied by using different amounts of propylphosphonic acid (PPA) and by the growth time. For example, Sample #4, which had the smoothest surface and smallest width of all, was grown using 25 mg of PPA and growth time of 20 min. More bumpy morphologies such as Samples 1 and 2 were obtained by using lower concentration of PPA and extending the growth time to 40 min.

An estimate of nanocrystal sizes from TEM images gave the following parameters: Sample 1: diameter 5 nm, length 50–60 nm, original CdSe seed diameter 4.1 nm; Sample 2: diameter 5.5 nm, length 50–60 nm, original CdSe seed diameter 3.1 nm; Sample 3: diameter 5 nm, length 20–30 nm, original CdSe seed diameter 5.1 nm; Sample 4: diameter 4.5 nm, length 40–50 nm, original CdSe seed diameter 3.5 nm.

Time-Resolved Photoluminescence: Optical excitation was provided by 150 fs pulses from a frequency-doubled Titanium:sapphire regenerative amplifier (Quantronix Integra C) with 3.1 eV photon energy and 1 kHz repetition rate. Laser pulses were focused down to a 130-μm spot on the nanocrystal solution. Photoluminescence was measured with a C5680 Hamamatsu streak camera. The temporal resolution in the configuration we employed was ~100 ps. Decay traces were extracted from streak-camera spectrograms by integrating over a ~50-nm-wide spectral window that included both exciton and biexciton emission.

Transient Absorption: The absorption spectrum was probed with white-light continuum 150 fs long laser pulses, 450 nm to 700 nm in spectrum, generated by focusing the output of the regenerative amplifier (Quantronics Integra), attenuated to approximately 1 μJ energy per pulse, on a 1-mm-thick sapphire plate. Probe pulses had a variable delay with respect to pump pulses (394-nm wavelength, 150 fs long, same as photoluminescence excitation). Pump and probe beams (1mm in waist) crossed with a ~5° relative angle on a 1-mm-thick quartz cuvette filled with nanocrystals dispersed in toluene. The cumulative effect of spectral chirp and wavefront distortion of laser pulses resulted in a 200 fs time-delay resolution for experiments. The concentration of nanocrystals was chosen to keep the optical density of the whole cuvette around 0.3 at 400 nm in wavelength, guaranteeing the best compromise between uniformity of excitation and magnitude of the absorption signal. Optical spectra were recorded with a CCD camera (Princeton Instruments VersArray) coupled to a grating spectrometer (Acton SP2500i). Sample transmission was measured by dividing the spectrum of white-light pulses sent through the sample by the spectrum of similar pulses split before reaching the sample. Differential transmission $\Delta T = (T_{on} - T_{off})/T_{off}$ was obtained by recording sequential transmission spectra with (T_{on}) and without (T_{off}) pump pulses illuminating the sample. Typical sensitivity to differential absorption changes in our set-up was about 2×10^{-4}. Absorption and differential absorption spectra could be traced back through the relation linking absorption α and transmission T, when reflection and scattering are neglected: $\alpha = 1 - T$. The linear absorption α_0 was instead measured with a spectrophotometer. We estimated an uncertainty of about 10% on the absolute value of α_0 at 610 nm, as a result of noise and offset fluctuations affecting the linear absorption measurement at very low absorbance values. Such uncertainty is propagated to differential absorption values $\Delta\alpha/\alpha_0$.

Acknowledgements

Funding for this work was partly provided by the grant ''Rientro dei cervelli'' from the Italian MIUR, INFM-CNR Seed project for young researchers, FIRB-MIUR project Synergy-FIRBRBNE03S7XZ, European Commission through the Human Potential Programs (RTN Nanomatch, Contract No. MRTN-CT-2006-035884), Austrian Nano-Initiative (project NSI), Austrian Science Fund FWF (project START Y179), and NSF MRSEC Program under Award Number DMR-0213745. Supporting Information is available online from Wiley InterScience or from the author.

Received: May 5, 2009
Published online:

[1] C. B. Murray, C. R. Kagan, M. G. Bawendi, *Annu. Rev. Mater. Sci.* **2000**, *30*, 545.
[2] *Semiconductor and Metal Nanocrystals: Synthesis and Electronic and Optical Properties*, (Ed: V. I. Klimov), Marcel Dekker, New York **2003**.
[3] Y. Yin, A. P. Alivisatos, *Nature* **2005**, *437*, 664.
[4] G. Konstantatos, I. Howard, A. Fischer, S. Hoogland, J. Clifford, E. Klem, L. Levina, E. H. Sargent, *Nature* **2006**, *442*, 180.
[5] V. I. Klimov, A. A. Mikhailovsky, S. Xu, A. Malko, J. A. Hollingsworth, C. A. Leatherdale, H.-J. Eisler, M. G. Bawendi, *Science* **2000**, *290*, 314.
[6] A. Piryatinski, S. A. Ivanov, S. Tretiak, V. I. Klimov, *Nano Lett.* **2007**, *7*, 108.
[7] V. I. Klimov, S. A. Ivanov, J. Nanda, M. Achermann, I. Bezel, J. A. McGuire, A. Piryatinski, *Nature* **2007**, *447*, 441.
[8] D. V. Talapin, R. Koeppe, S. Goetzinger, A. Kornowski, J. M. Lupton, A. L. Rogach, O. Benson, J. Feldmann, *Nano Lett.* **2003**, *3*, 1677.
[9] D. V. Talapin, J. H. Nelson, E. V. Shevchenko, S. Aloni, B. Sadtler, A. P. Alivisatos, *Nano Lett.* **2007**, *7*, 2951.
[10] L. Carbone, C. Nobile, M. De Giorgi, F. D. Sala, G. Morello, P. Pompa, M. Hytch, E. Snoeck, A. Fiore, I. R. Franchini, M. Nadasan, A. F. Silvestre, L. Chiodo, S. Kudera, R. Cingolani, R. Krahne, L. Manna, *Nano Lett.* **2007**, *7*, 2942.
[11] a) B. O. Dabbousi, J. Rodriguez-Viejo, F. V. Mikulec, J. R. Heine, H. Mattoussi, R. Ober, K. F. Jensen, M. G. Bawendi, *J. Phys. Chem. B* **1997**, *101*, 9463. b) X. Peng, M. C. Schlamp, A. Kadavanich, A. P. Alivisatos, *J. Am. Chem. Soc.* **1997**, *119*, 7019.
[12] J. Muller, J. M. Lupton, A. L. Rogach, J. Feldmann, D. V. Talapin, H. Weller, *Phys. Rev. Lett.* **2004**, *93*, 167402.
[13] J. Muller, J. M. Lupton, P. G. Lagoudakis, F. Schindler, R. Koeppe, A. L. Rogach, J. Feldmann, D. V. Talapin, H. Weller, *Nano Lett.* **2005**, *5*, 2044.
[14] R. M. Kraus, P. G. Lagoudakis, A. L. Rogach, D. V. Talapin, H. Weller, J. M. Lupton, J. Feldmann, *Phys. Rev. Lett.* **2007**, *98*, 017401.
[15] Such decay appeared shorter than the one observed in the low-excitation photoluminescence in Figure 2a because we could not lower the excitation level as much and still have a detectable signal (0.2 excitons/dot produced $\sim 10^{-3}$ differential transmission signal, with our sensitivity at $\sim 2 \times 10^{-4}$).
[16] M. Achermann, J. A. Hollingsworth, V. I. Klimov, *Phys. Rev. B* **2003**, *68*, 245302.
[17] a) J.-M. Caruge, Y. Chan, V. Sundar, H. J. Eisler, M. G. Bawendi, *Phys. Rev. B* **2004**, *70*, 085316. b) B. Fisher, J.-M. Caruge, Y. T. Chan, J. Halpert, M. G. Bawendi, *Chem. Phys.* **2005**, *318*, 71.
[18] D. Oron, M. Kazes, U. Banin, *Phys. Rev. B* **2007**, *75*, 035330.
[19] A 1D particle-in-a-box calculation of electron and hole wavefunctions for our dot/rod nanocrystals gave an overlap factor for electron and hole wavefunctions in excess of 0.9. Electron and hole masses in CdSe are respectively 0.12 *me* and 0.45 *me*; conduction and valence band offsets are 0.27 eV and 0.51 eV, respectively.
[20] M. G. Lupo, F. Della Sala, L. Carbone, M. Zavelani-Rossi, A. Fiore, L. Lüer, D. Polli, R. Cingolani, L. Manna, G. Lanzani, *Nano Lett.* **2008**, *8*, 4582.
[21] D. Steiner, D. Dorfs, U. Banin, F. Della Sala, L. Manna, O. Millo, *Nano Lett.* **2008**, *8*, 2954.
[22] Purchased from Evident Technologies, inc. Nominal radius was 5.8 nm, luminescence emission peak at 620 nm.
[23] Y. Yang, G. A. Turnbull, I. D. W. Samuel, *Appl. Phys. Lett.* **2008**, *92*, 163306.
[24] J. Li, L.-W. Wang, *Nano Lett.* **2003**, *3*, 1357.